

## Hidden Transition in the “Unfreezable Water” Region of the PVP–Water System

Michiel J. A. de Dood, Jeroen Kalkman, Chris Strohhofer, Jan Michielsen, and Jan van der Elksen\*

FOM Institute for Atomic and Molecular Physics, Kruislaan 407, 1098 SJ Amsterdam, The Netherlands

Received: September 26, 2002; In Final Form: January 27, 2003

Poly(vinylpyrrolidone)–water solutions of 60–80 wt % PVP apparently do not freeze when cooled far below the expected freezing point. Such solutions remain highly viscous liquids and ultimately become glasses. It has been reported before that when small-angle X-ray scattering from these solutions is measured, occasionally very sharp peaks appear. The collection of those peaks, that have, in general, a short lifetime, constitutes a hexagonal planar reciprocal lattice. We present new, extensive small-angle scattering measurements, from which we are able to collect statistically relevant numbers of such peaks. This will allow us to infer more about their origin. The scattering results that are obtained on low concentration solutions show the existence of wavy layer structures, which may have a connection with a hexagonal structure at higher concentration. Most important is, however, that we found that the scattering spectra, time averaged in frames of 30 s or more, show a pronounced time dependence, be it over hours. The rate of change increases with decreasing temperature. Surveying the possible causes of such a dependence, we were led to the conclusion that, in the concentration range considered, the systems are not in equilibrium. In a narrow region of temperature, molar weight, and concentration, the system is still visibly in the process of phase separation. The underlying mechanism is considered.

### Introduction

Poly(vinylpyrrolidone) (PVP)–water solutions have been much investigated because of their peculiar behavior at temperatures below the normal freezing point of water.<sup>1</sup> The liquidus of the temperature versus composition ( $T-x$ ) binary phase diagram that is usually shown seems to start in a perfectly normal way at low concentration but bends sharply downward at higher concentrations and apparently becomes vertical at a concentration of about 57 wt % polymer.<sup>1,2</sup> Presumably, the liquids of higher concentration remain liquid at low temperatures, till finally these form a glass: PVP does not crystallize from the aqueous solutions, and ice does not crystallize from solutions of concentrations higher than 57 wt %. From vapor pressure measurements<sup>2</sup> it is clear that, in such high concentration solutions, water does not act as a solvent in the usual sense. It is customary to speak of “bound” water, although it is not always clear whether this is meant in a thermodynamic or in a kinetic sense. There is quite some information about the PVP–water system at temperatures down to 230 K in the two-phase region at concentrations up to 57 wt % polymer.<sup>1</sup> About the high concentration solutions, less is known. Still one might well wonder whether the visibly clear liquid of 60 or 70 wt % hides a structure, and if so, whether it is in a metastable state or not in equilibrium at all. Electron micrographs of samples that were temperature quenched into a solid state and fractured show a gnarled texture on a 10 nm scale. It has been surmised that, in the liquid at higher temperatures, a similar structure might be present.<sup>1</sup>

In earlier X-ray scattering experiments, in the small-angle region,<sup>3</sup> we noted that a solution of more than about 60 wt % PVP in water, be it of molecular weight 10 000 or 40 000 g mol<sup>-1</sup>, measured at a temperature of 263 K, gives rise to a

scattering curve with an intensity that continuously increases with decreasing scattering vector, provided that one time averages the scattering in frames of 30 s or more. The continuous increase persists up to the smallest scattering vector that we could experimentally attain. Furthermore, it seemed that the overall intensity depends on the temperature.

On top of this smooth scattering curve, occasionally very sharp peaks appear, that however have only a lifetime on the order of seconds and will therefore only appear as such when the scattering is measured in very short time frames. Moreover, in one very fortunate, if not fortuitous, run, it appeared that the values of the scattering vectors had ratios that corresponded with the values of the Bragg peaks associated with a two-dimensional hexagonal reciprocal lattice, that is,  $\sqrt{3}$ ,  $\sqrt{7}$ ,  $\sqrt{9}$ ,  $\sqrt{13}$ , and so forth.<sup>3</sup> The appearance of such a pattern seemed to be rather unique. One could wonder whether the observation was just caused by a chance event or it was a reflection of events that under different conditions, such as temperature or concentration, are part of normal system properties. It should be noted that, judged by the width of the peaks, the size of the scattering objects could have been as much as 500 nm. A closer investigation into the scattering properties of the PVP–water solutions seemed necessary to find an answer to two main questions. The first question is what sort of structure grows on cooling and is there a relation between the hexagonal pattern and the structure observed in the electron micrographs. The second is what could the cause be of a temperature dependence of the total scattering intensity.

### Experimental Section

Solutions were made of PVP obtained from Polysciences,  $M = 10\,000$  (number-average molar mass  $M_N = 2500$  and weight-average molar mass  $M_W = 7\,000$ – $11\,000$ ) and  $M = 40\,000$

\* Correspondence e-mail: library@amolf.nl.

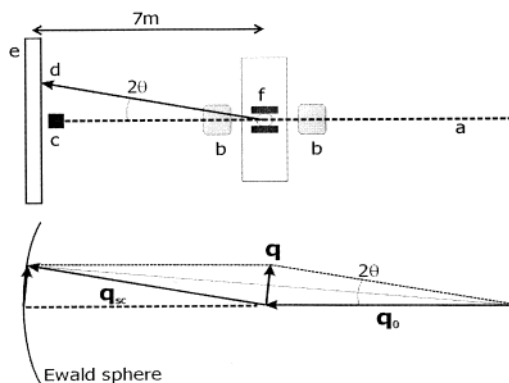


**Figure 1.** Schematic drawing of the measurement geometry (upper part): (a) primary beam; (b) ionization chambers; (c) beam stop; (d) scattered beam; (e) two-dimensional wire detector; (f) Peltier elements cooling the sample. The corresponding vector diagram, which defines the Ewald sphere (lower part), with the  $\mathbf{q}$ -vector of the primary beam  $\mathbf{q}_0$ , that of the scattered beam  $\mathbf{q}_{sc}$ , and the scattering vector  $\mathbf{q}$ .

( $M_N = 12\,000$  and  $M_W = 44\,000$ – $54\,000$ ), all in grams per mole.

A small drop of the solution was held between two shallow brass cups, which could be cooled with the aid of two Peltier elements, down to about 243 K, Figure 1. The distance between the cups could be varied in such a way that an approximately cylindrical drop, 5 mm diameter and 5 mm height, of free surface was obtained. The windowless cell was shielded from the surroundings by a polycarbonate housing, which was flushed by dry nitrogen gas. Two thin Mylar windows admitted the X-ray beam; the scattering by these windows is negligible. The liquid in the drop, although highly viscous, is free to move and will do so under the influence of the temperature gradients set up by the cooling.

Small-angle X-ray scattering (SAXS) was measured at the DUBBLE beam line of the ESRF in Grenoble. In the experimental configuration the primary beam went through the drop and was caught by a beam stop in front of the detector. The two-dimensional multiwire gas filled detector, surface 133 mm  $\times$  133 mm, recorded the intensity of the scattered radiation that was not intercepted by the beam stop, which was about 5 mm  $\times$  5 mm. The intensities were normalized with the aid of two ionization chambers, one before and one after passage of the beam through the sample. The scattered intensity is recorded, as a function of the angle  $2\theta$  between the scattered beam and the direct beam. This defines a scattering wave vector, modulus  $q = (4\pi/\lambda) \sin \theta$ , with  $\lambda$  the wavelength of the X-rays, mostly 0.146 nm. In Figure 1 it can be seen that in the small-angle geometry the relevant part of the Ewald sphere is directly mapped out on the plane of the detector. The beam stop and the distance between sample and detector, which is variable, limit the total measurable  $q$ -range. With a distance of 3000 mm, the shortest wave vector at which a peak could be detected was  $0.15\text{ nm}^{-1}$ . For a reliable intensity measurement,  $0.2\text{ nm}^{-1}$  was the limit, because of spurious radiation caused by the proximity of the beam stop. In a special instrumental arrangement, a curved delay line detector allowed us to measure the normal wide-angle scattering simultaneously.<sup>4</sup>

## Results and Discussion

The sharp peaks in the scattering spectrum, on which we reported before,<sup>3</sup> were interpreted as arising from a hexagonal, columnar structure. It seemed mandatory to collect the values of the scattering vectors of a great many of such peaks, and so

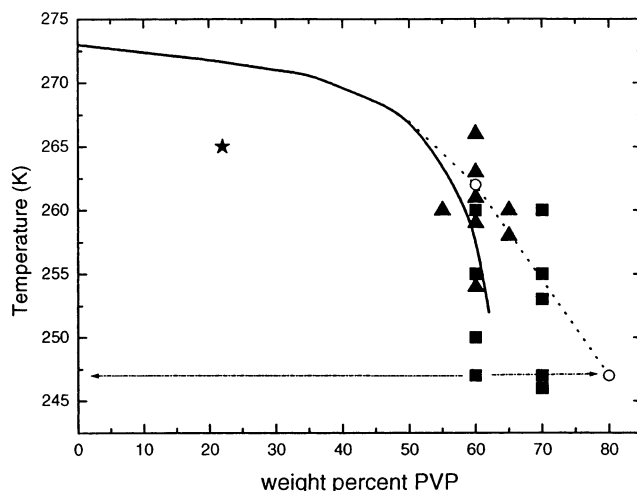


**Figure 2.** Summary of the concentration and temperature of the measurements. The star, ★, indicates a rather wide area in which layer structures have been found. Triangles, ▲, indicate measurement of short-time frames which gave isolated peaks. Squares, ■, are measurements of long time frames with the aim to find the temperature and time dependence of the scattering. The drawn line is the phase line, as has been suggested in the literature.<sup>1,2</sup> The open circle, ○, gives the concentration at 248 K, which should be in equilibrium with ice, according to the findings of this paper. The dashed line is the approximate phase line which connects the equilibrium points at 262 K, 60 wt %, and 248 K, 80 wt %.

establish the reproducibility and corroborate the interpretation. Figure 2 shows the concentrations and temperatures of the solutions that were investigated. In the measurements that we performed, the handpicked “peaks” are counted as such, when the local intensity exceeds about three times the noise level. In total we collected about 600 values, from five thousand frames of 1 s and more than two thousand frames of 15 s. It turned out that there are two kinds of peaks. Some of the observed peaks are persistent inasmuch that the value of the scattering vector appears in many successive frames or moves in time in radial directions. Such peaks are often part of a radial ridge of somewhat higher intensity. The other peaks appear only during a short time and stand isolated in  $q$ -space. Figure 3 shows an arbitrary example of a 15 s frame; Figure 4 summarizes the result of a 1 h measurement on a 60 wt % PVP ( $M = 10\,000$ ) at 260 K. The  $x$ - and  $y$ -axes correspond with the axes of the two-dimensional detector, and the  $z$ -axis corresponds with the time. All points are projected onto the bottom plane. One easily recognizes the more persistent points that form “streaks”. The solitary points in the figure represent the peaks that appear only in one or in a few 15 s frames.

**Columns.** The group of points that appear for a short time only have been collected in a histogram, shown in Figure 5. Most points were collected from 60 wt % solutions, but points from 55 wt % and 65 wt % solutions are also included, as shown in Figure 2. The product of incidence and intensity has been weighted by the absolute value of the wave vector. It is seen that the maxima in the histogram again corresponds with the two-dimensional hexagonal reciprocal lattice. The combined occurrence of peaks corresponds with  $\sqrt{3}$ ,  $\sqrt{7}$ ,  $\sqrt{13}$ ,  $\sqrt{19}$ ,  $\sqrt{21}$ ,  $\sqrt{28}$ , and  $\sqrt{31}$  times  $0.144 \pm 0.003\text{ nm}^{-1}$ , following  $(h^2 + k^2 - hk)^{1/2}$ , while reckoning with the multiplicity factor. This pattern is characteristic for a hexagonal columnar structure in real space, with a lattice spacing of  $43 \pm 1\text{ nm}$ . Although more points may simultaneously appear in the same frame, hexagonal relations such as  $120^\circ$  angles between them are rarely seen. Mirror images,  $180^\circ$  relations, however, are frequent. This can

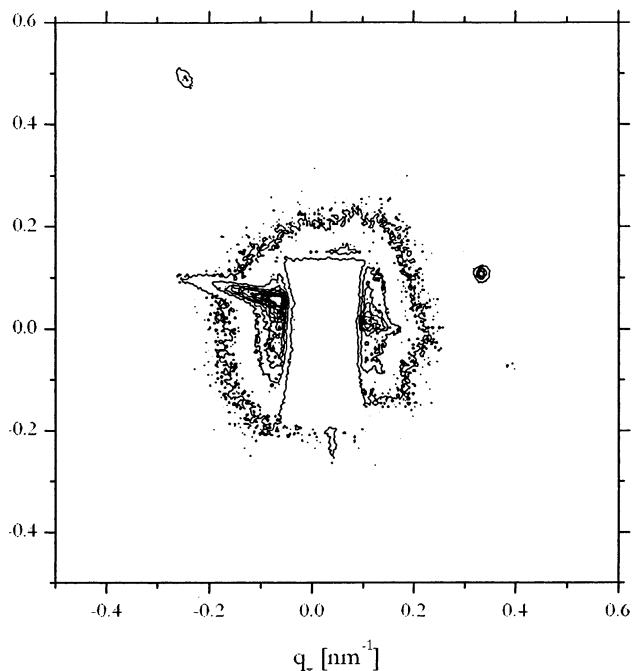


**Figure 3.** Contour plot of the scattered intensity from a 60 wt % solution of PVP ( $M = 10\,000$ ) in water at a temperature of 255 K. It shows clearly the intensity ridge caused by an interface, as well as two isolated points of high intensity.

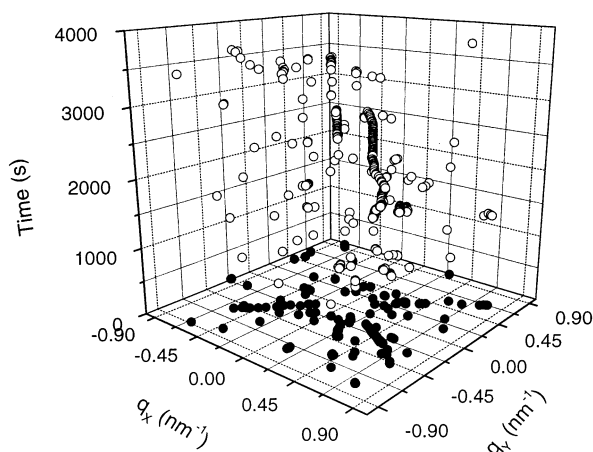


**Figure 4.** Result of a single, 1 h run of a 60 wt % PVP solution at 263 K presented as a three-dimensional plot of the coordinates of spots of relatively high intensity (open circles), which were found in 256 consecutive frames of 15 s each. The  $x$ - and  $y$ -axes ( $q$  space) correspond with the  $x$ - and  $y$ -axes of the two-dimensional detector, the  $z$ -axis corresponds with the time. To assist in the interpretation of the figure, we projected all points on the  $x$ - $y$  plane (filled-in circles). The projected figure could be considered as a picture of a long time frame. One can recognize that “snakes”, as in the upper right of the spatial figure, tend to form “streaks” in figures obtained with long time frames.

be understood if one considers that only those points give rise to positive interference that are situated on the line of intersection of the reciprocal lattice, which is plane hexagonal, and the Ewald sphere, which is almost planar in the  $q$ -range covered by SAXS. Only when the planes coincide could one expect to see a hexagonal pattern, a rare event indeed.

A plane, hexagonal, reciprocal lattice can find its origin in two entirely different situations in real space. The first possibility is that columns of PVP are formed independently. When such columns float in water or in a dilute solution of PVP in water, they may pack together in a hexagonal way. The other possibility

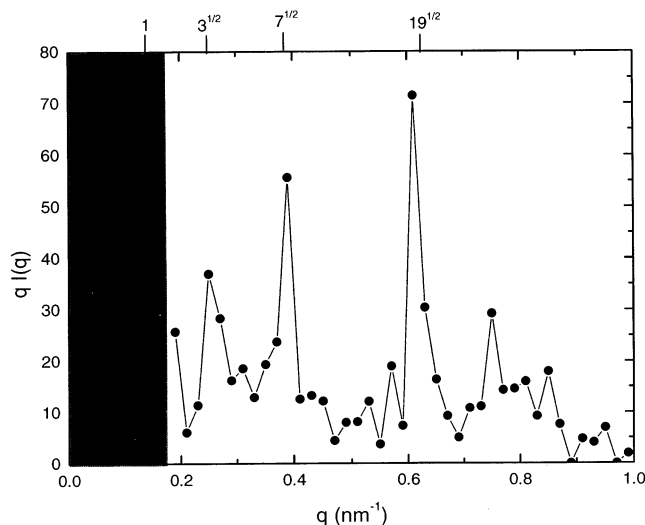


**Figure 5.** Histogram which shows the weighted sum of the peak intensities as a function of the scattering vector. The observations were made in six runs, in total about 10 hours. The maxima are centered at  $q$  vector values that have ratios  $\sqrt{3}$ ,  $\sqrt{7}$ ,  $\sqrt{19}$ , and possibly  $\sqrt{28}$ .

is that, in a locally, nematic order PVP, elongated cells are being formed with water (ice) as separating medium, resulting in a hexagonal pattern of intercalated water in a continuum of polymer. Both situations have been reported as appearing in polymer solutions.<sup>5,6</sup> In the latter case, the hexagonal pattern would be the final situation after a process in which the cross section,  $\varnothing$ , of the cells, that may at first be of irregular shape with less than six sides, grows according to von Neumann's rule,<sup>7</sup>  $d\varnothing/dt = C(n - 6)$ , where  $n$  is the number of sides.

In the case of independent columns, a very limited number that stick together in a parallel fashion could already give rise to local maxima in the scattering curve. Peaks associated with high Miller indices would of course not appear, but even only six columns, drifting together, might give a  $\sqrt{3}$  maximum, while a sheaf of 24 columns is needed to give a  $\sqrt{7}$  peak, at a wave vector  $k = 0.40\text{ nm}^{-1}$ , and a width of only  $0.02\text{ nm}^{-1}$ , following the Scherrer equation,  $B(2\theta) = 0.94\lambda/L \cos \theta$ . The  $\sqrt{28}$  and  $\sqrt{31}$  peaks, originating from high indices, can only show up if lattices of at least 96 units are present.

The same consideration holds for cells of PVP with intercalated water. The conclusion that can be drawn from the appearance of local maxima in the scattering spectra and from the observed  $q$  values thereof should therefore mainly be that, in the PVP–water solutions of a concentration of 57 wt % and higher, columnar units of a diameter of about 40 nm might group themselves in a hexagonal structure. The more ephemeral character of clusters of independent columns is in good agreement with the incidental character of the observed peaks. On the other hand, the 6% spread of the values of the basic distance, following from Figure 5, could be seen as an argument in favor of the interpretation in terms of a more approximate hexagonal pattern in a moving continuum of polymer.

**Layers.** The more persistent peaks that we observed in the solutions of 60 wt %, at 260 K, have a different origin. The wave vectors at which the points of one of such “streaks” occur have been plotted versus the time of observation in the inset of Figure 6. The figure shows the continuous shift of the position of the peak maximum, back and forth over an almost straight line on the 2D detector. This proves that it is a single object that causes a moving point on the Ewald sphere. Such behavior is consistent with a plane interface slowly tumbling through

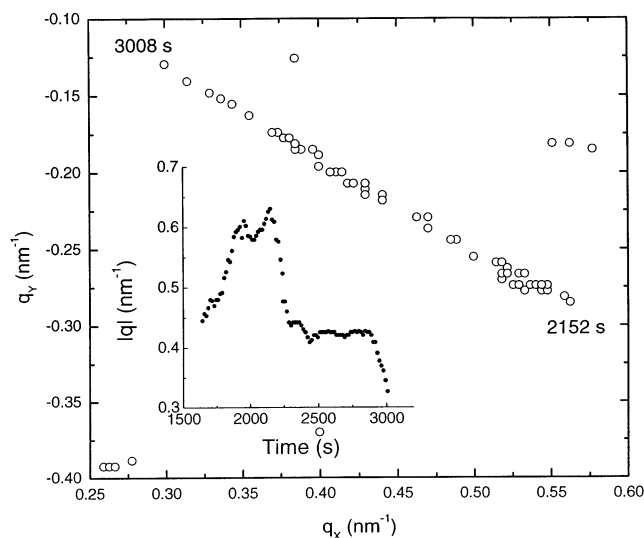


**Figure 6.** Coordinates of the maximum intensity peaks, which form the “snake” in Figure 4. In the inset is shown the modulus of the scattering vector as a function of time. The variation in the angle of the normal to the interface with the incoming beam is only  $0.19^\circ$ .

real space. In reciprocal space this corresponds with a rod, which makes a varying angle  $\alpha$  with the incoming beam, following the orientation in real space. In the Ewald construction it is represented by a line, which starts at the end point of the vector  $\mathbf{q}_0$ , representing the incoming beam. The line pierces the Ewald sphere, thus defining the end point of the scattered beam  $\mathbf{q}$ . The scattering vector  $\Delta\mathbf{q}$  has the length of the chord  $\Delta q = 2q_0 \sin \theta$ . Since  $\theta$  is the complement of  $\alpha$ , it follows that  $d\Delta q/d\alpha = -2q_0 \sin \alpha$ . In the example of Figure 6, the scattering vector changes between  $0.35$  and  $0.63 \text{ nm}^{-1}$  in  $1400 \text{ s}$ . Since  $\alpha$  is close to  $90^\circ$ , and the wavelength is  $0.148 \text{ nm}$ , the variation of the angle  $\alpha$  must have been  $0.0033 \text{ rad}$ , or only  $0.19^\circ$ . Such slow variation must find its origin in the movement of an interface within the drop of liquid and not in any motion at a molecular scale. A similar small variation in the angle perpendicular to the plane through the rod and the incoming beam would result in an equal small variation in the direction of the “streak” in the scattering image and would go undetected. The observation that we made here does therefore not mean that the motions in the drop would not be isotropic.

In dilute solutions of  $20\text{--}30 \text{ wt } \%$  PVP we find, in  $30 \text{ s}$  frames, similar ridges of high scattering intensity. The intensity variation along the ridge is characteristic of a structure of alternating layers of different contrast. A cosine transformation<sup>8</sup> of the intensity variation along the ridge gives the repeat distance  $L$  and an approximate thickness  $d$  of the layers. Typical values range from  $L = 10 \text{ nm}$  for a  $20 \text{ wt } \%$  solution to  $L = 35 \text{ nm}$  for solutions with concentrations up to  $35 \text{ wt } \%$ . The variation and uncertainty in the determination of  $d$  is large; it is on the order of  $10 \text{ nm}$ .

In some cases we also find clear evidence for the formation of undulating layers.<sup>9</sup> Figure 7 shows an example from which we deduce a repeat distance  $L$  of the layers of approximately  $13 \text{ nm}$ , whereas the undulation has a wavelength of  $150 \text{ nm}$  and an amplitude of  $5 \text{ nm}$ .

For such a laminar structure to be locally in equilibrium, the attractive force and the repulsive force between two PVP layers separated by a water layer have to be equal. The attractive force is equal to  $H_A/6\pi r^3$ , where  $H_A$ , the Hamaker constant, is assumed to be about  $10^{-21} \text{ J}$ . The hydration repulsive force has an exponential form,  $c \exp(-r/\xi)$  involving a correlation length  $\xi$  as an unknown parameter. Inserting appropriate values for

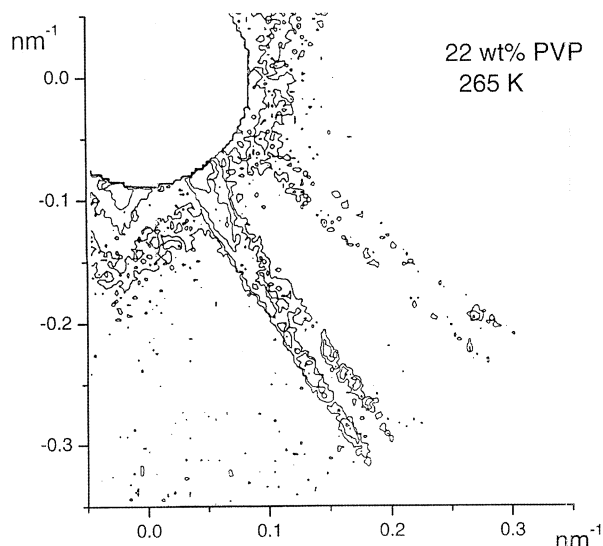


**Figure 7.** Contour plot of the scattered intensity of a  $22 \text{ wt } \%$  PVP solution in water, at  $265 \text{ K}$ . The two double ridges at an angle of  $22^\circ$  correspond with an undulating layer structure.<sup>9</sup>

the dipolar surface charge density and dielectric constants in the constant  $c$ , one can calculate the repulsive forces for different values of  $\xi$ . It turns out that equilibrium distances between  $5$  and  $10 \text{ nm}$  are found with correlation lengths between  $0.09$  and  $0.18 \text{ nm}$ , which are reasonable values similar to those found in phospholipid bilayers.<sup>10</sup> It is therefore quite possible that the observed laminar structures are near equilibrium.

Transitions of lamellar to hexagonal tubular structures have been described before.<sup>11</sup> In many cases, water is presumably intercalated as sheets or as tubular channels, in the polymer continuum. The undulating layers in low concentration solutions, and the hexagonal structures in PVP solutions of higher concentration, may be connected in this way. If the layer structure consists of alternating layers, of water and of PVP with bound water, a plane wave pattern with a  $180^\circ$  phase shift between successive layers could be excited. If, now, the amplitude reaches a magnitude of half the thickness of the PVP–water layer, minimalization of the surface tension might stabilize a hexagonal columnar pattern. For a space filling structure of hexagonal columns of  $35 \text{ nm}$ , separated by  $10 \text{ nm}$  of water, the volume ratio is  $1.5$ . Ignoring the unknown density differences, this corresponds with a concentration of  $60 \text{ wt } \%$  PVP, remarkably close to the divergence in the phase diagram! Of course, it is more likely that undulating laminar structures give rise to columns, two-dimensionally bundled in an irregular pattern of polygons. Surface tension will subsequently cause a process like Ostwald ripening. Thicker columns will grow at the expense of thinner ones, as far as the water–PVP ratio will permit. Moreover, according to von Neumann’s rule,<sup>7</sup> columns with less than six edges will disappear. The final result is the same.

**Dependence on Temperature and Time.** The appearance of the sharp features in the frames of short duration is a rare event. Even in runs lasting  $10 \text{ h}$  the statistics is not good enough to quantify a dependence on temperature. However, in long time frames of  $30 \text{ s}$  or more, the sharp features become time averaged. The smooth, averaged scattering spectrum has roughly the form  $(a + bq^2)^{-1}$ . We noticed that the overall intensity starts growing with time when the temperature is lowered below  $262 \text{ K}$ . The low  $q$  side of the spectrum increases far more than the high  $q$  side; in some cases we could ascertain a decrease at scattering vectors larger than about  $0.6 \text{ nm}^{-1}$ . Such behavior is charac-

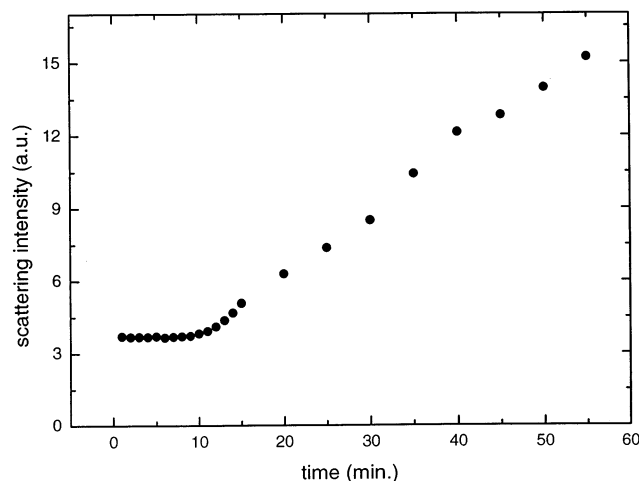


**Figure 8.** Intensity of the scattering at  $q = 0.231 \text{ nm}^{-1}$ , during 1 h after a temperature quench to 251 K, from a solution of 60 wt % PVP ( $M = 10\,000$ ) in water.

teristic for a first-order transition of a nonequilibrium system that approaches equilibrium by some form of phase separation.<sup>12</sup> The velocity of such a process may increase with decreasing temperature, because the driving force, which is the difference in thermodynamic potential, increases. Furthermore, the order parameter involved in the description of the transition may be conserved, such as a concentration deviation, or nonconserved. In the latter case there should be some coupling with a locally conserved variable such as density to provide a connection with experimental observation. It is not a priori clear what the character of the changes in the PVP–water system is. It could be a simple first-order phase separation. It could also be a more complicated order–disorder transition, involving the columnar structures.

To come to a more quantitative assessment of the possibilities, we applied quenches to different temperatures and to solutions of different concentration; see Figure 1. After the quench, we followed the scattering spectra for 2 h, taking frames of 30 s during the first 15 min and frames of 300 s after that.

In Figure 8, the intensity of the scattering at  $q = 0.103 \text{ nm}^{-1}$ , of a 60 wt % solution, is plotted versus the time. To reach the quench temperature, here 251 K, takes about 1 min. One notices four time intervals in which the time dependence is very different. The first 8 min, nothing seems to happen at all. Then there is for about 10 min a rapid increase of the intensity. Thereupon, the intensity growth slows down, and for the duration of the measurement, the intensity increases roughly linearly with time. In some runs, after about 1 h, the intensity started to change in an erratic way.

Qualitatively one can understand the successive stages as follows. As soon as the system finds itself in an unstable state, a reorganization at a molecular length scale sets in. In the small-angle scattering region this will not be visible. As soon as the length scale reaches a critical value, we see in the changes of the scattering function the time evolution of the order parameter. In the long time limit, the time evolution reflects the growth of large domains of the new phase, at the cost of the smaller domains. Finally, in the last time regime, the domains have grown to a size comparable with the size of the footprint of the X-ray beam. The liquid of the sample, although very viscous, may move, because of the hydrodynamic instability that can be induced by the cooling Peltier elements. Different parts of the liquid will cross the beam and give rise to the erratic behavior that is observed.

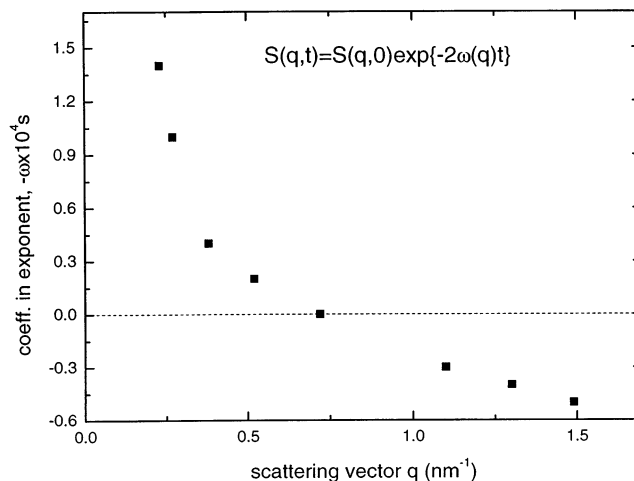


**Figure 9.** Coefficient  $\omega(q)$  in the exponent of the initial growth rate  $S(q,t) = S(q,0) \exp\{-2\omega(q)t\}$  versus the wave vector  $q$ . The experimental points are from a 60 wt % PVP solution quenched at 250 K and are not quite in agreement with what one would expect from a spinodal decomposition. A possible maximum in the curve could be situated at such a low  $q$  vector that it is hidden behind the beam stop.

**Is It a First-Order Transition?** Field-theoretic theories<sup>12</sup> do indeed predict an exponential change of the scattering function,  $S(q,t) = S(q,0) \exp(-\omega(q)t)$ . The dependence of  $\omega$  on  $q$  is determined by the particulars of the model that is used. The exponential growth may gradually diminish toward higher  $q$  values, or there may be a maximum growth at finite  $q$  and a transition to negative growth at higher  $q$  values. In the latter case, there should be a maximum at finite  $q$  in the final scattering curve as well. This is characteristic for a transition with a conserved order parameter. A scattering curve that rises continuously with decreasing  $q$ , approaching  $q = 0$ , may be associated with a nonconserved order parameter. By plotting the logarithm of the experimental intensity at different values of the scattering vector, versus time, during the 10 min of the exponential growth, we obtained  $\omega(q)$ . The result for a 60% solution at 250 K is shown in Figure 9 as an example. It is not in accordance with any of the simple models for critical dynamics.<sup>12</sup> It is disappointing that no firm conclusion can be drawn about the presence or absence of a maximum in the  $\omega(k)$  curve. The necessary information might well be hidden behind the beam stop. In this way, we cannot decide about the character of the order parameter or about an approximate length scale. To assess the character of the transition, we must therefore refer to the later stage, that starts after about 20 min and looks like the coarsening regime of a phase separation process. Domains of the phase that is being formed are growing, the larger ones at the expense of the smaller.

**Length Scale  $L$ .** To quantify this behavior, one usually takes the length scale of the maximum of the size distribution. In the absence of that information, we can extract a relative length scale. One assumes that the scattering functions obey the dynamical scaling hypothesis, which states that a single characteristic length scale,  $L(t) = \kappa(t)^{-1}$ , determines the structure function.

The scattering  $I(q,t)$  is proportional to the structure function  $\hat{S}(q,t)$ . We can normalize  $\hat{S}(q,t)$  by dividing by the second moment, and so define  $\tilde{S}(q,t) = \hat{S}(q,t)/\{\Sigma q^2 \hat{S}(q,t)\}$ . The scaling assumption is that, after an initial time, the function  $\tilde{S}(q,t) = \kappa^{-d} F(q/\kappa(t))$ . When we now identify  $\kappa$  as the square root of the second moment, the simplest reciprocal length scale at hand, we are able to write  $F(q/\kappa) = \kappa^d \kappa^{-2} \hat{S}(q,t)$ , so that, for the dimension  $d = 3$ , we obtain  $I(q,t) \sim \hat{S}(q,t) = \kappa^{-1} F(q/\kappa)$ .

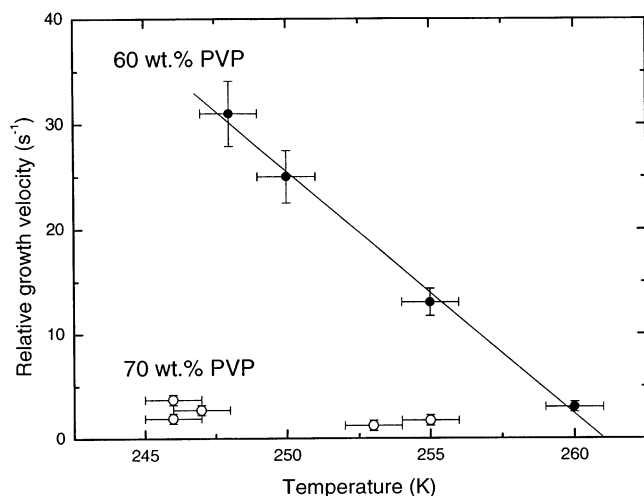


**Figure 10.** Growth rate of the characteristic length, plotted as  $L(t,T)^3/L(0,T)^3$  versus the temperature. The data for the 60 wt % solutions clearly rise about linearly with temperature, starting at 262 K. The rates for the 70 wt % solutions are too low to draw that conclusion.

The scaling procedure can now be applied to our experimental data. One contracts the wave vector scale and expands the intensity scale of the scattering function with the same time dependent factor, till the functions coincide for all times. It works well over a large  $q$ -region. The procedure supplies us with a possibility to represent the time and temperature dependence of the scattering spectra as the dependence of one, single parameter  $L(t,T)/L(0,T)$ . Considering the introduction of  $L$  as  $\kappa^{-1}$ ,  $\kappa$  being the square root of the second moment, one could obtain an absolute value of the characteristic length if one could determine the values of the second moment, preferably at  $t = 0$ . Unfortunately, there is a lack of data on important parts of the low, as well as of the high,  $q$  side of the scattering function. This means that experimentally only a rough estimate of the magnitude can be obtained. The scaling procedure provides us at least with accurate *relative* values. To connect the experimental results quantitatively with any model requires the value of  $L(0,T)$ . We estimated the value of the second moment at  $t = 0$ , resulting in an order of magnitude value of 100 nm for  $L(0,T)$ , regardless of the temperature.

**Time Dependence of  $L/L(0)$ .** The next step is the determination of the power of the time dependence of  $L(t,T)$ . The asymptotic ( $t \rightarrow \infty$ ) growth of droplets or grains of a minority phase in a supersaturated solution is particularly well established.<sup>13</sup> In that case, the average radius of the droplets,  $R_0$ , grows as  $t^{1/3}$ . In the following we will find that the scaling parameter  $L$  has indeed that time dependence. Therefore, a first-order transition is very probable.

The determination of the power  $1/3$  of the time requires a very precise determination of the zero time point. In the systems that we investigated, this did not pose a problem. The plots extend over 2 h or more, whereas the temperature equilibration took  $<1$  min. Runs that started long before, or runs that started well after, the temperature quench always indicated the  $t = 0$  moment very accurately when  $L(t,T)^3/L(0,T)^3$  was plotted against  $t$ .

The value of the slope of such plots for 60 and 70 wt % solutions is plotted versus the quench temperatures in Figure 10. The relative velocity of the growth changes from 13 for a 60 wt % solution at 255 K to 39 at 245 K. The 60 wt % data show a clear temperature dependence. Extrapolation gives 261 K as the temperature at which the velocity becomes zero. At higher temperatures, the system is stable. The data for the 70

wt % solutions are so much lower that the scatter in the data points makes further conclusions less clear.

**Thermodynamics.** We start by observing that evidently the system is in equilibrium at 261 K, as can be deduced from Figure 10. At temperatures below 261 K, the systems change more rapidly, the lower the temperature. This is typical for the approach to equilibrium of nonequilibrium systems, with an increasing driving force, as the difference in free energy between the actual and equilibrium state increases. We can approximately calculate these free energy differences.

We assume that the contribution to the free energy from mixing  $N_1$  molecules of water with  $N_2$  molecules of polymer can be described by a Flory–Huggins type function<sup>14</sup>

$$\Delta F_m = RT\{N_1 \ln \varphi_1 + N_2 \ln \varphi_2 + \chi N_1 \varphi_2\} \quad (1)$$

The  $\varphi_1$  and  $\varphi_2$  are the volume fractions of water and of polymer, and the parameter  $\chi$  is the specific free energy of interaction. The polydispersity of the PVP prevents a really quantitative elaboration of this form, which ought to be summed over all species present. Nonetheless, it can serve well to test the thermodynamic possibilities. We also ignore the contribution of interface terms to the free energy.

By taking the tangent to the curve, described by eq 1, taken at  $T = 261$  K, at a value of  $N_1$  corresponding with a 60 wt % PVP solution, we find as its intersection with the  $N_1 = 1$  axis the value of the molar free energy of the water phase, presumably ice, that is in equilibrium with the water in the solution. If we now adjust the curve to a different temperature, say 248 K, and correct the entropy term in the free energy of ice accordingly, the point of contact of the new tangent that we can construct gives us the concentration of the solution that will now be in equilibrium with ice. The vertical distance between the original point of contact and the new tangent at the original composition gives us the free energy difference  $\Delta F$  and hence the driving force.

There are two free parameters in this treatment, the ratio between the volume fractions and the value of  $\chi$ . The ratio follows from the slope of the tangent. It turns out that  $\varphi_1/\varphi_2 = N_1/rN_2$ , with  $r$  a rather high value of about 3000. This means that the water in the high concentration equilibrium PVP solution hardly contributes to the total volume, which is in accordance with the idea that a high fraction of the water is incorporated in the polymer chains.

The value of the parameter  $\chi$  should be of the order one. Without an interaction energy, the free energy increases 5% by changing the temperature from 261 to 248 K. Inserting a value for  $\chi$ , equal to 1, adds an extra 2% to this increase. The resulting free energy difference,  $\Delta F$ , constituting the driving force, can be estimated to be about 0.2 kJ mol<sup>-1</sup>.

It is of importance that the concentration at which the new point of contact of the tangent is found is not very sensitive for the precise value of the parameter  $\chi$ . This is a consequence of the extreme values of  $N_1$ , very close to 1. Therefore, the outcome of these considerations is that a 60 wt % PVP solution, in equilibrium at 261 K, when cooled to 248 K, separates off an extra amount of ice and forms a solution of about 80 wt %. This result has been introduced in Figure 2, together with a tentative phase line, which has a slope approximately corresponding with an enthalpy difference of 3.5 kJ mol<sup>-1</sup>. It means that 4 molecules of water, adsorbed per one monomer of PVP, are reduced to 1.5 molecules per monomer, and that it takes many hours to do so.

It should be mentioned that, in solutions of 70 wt % PVP  $M = 10\,000$  as well as in solutions of 60 wt % PVP  $M = 40\,000$ ,

the same processes might occur. The rates will be an order of magnitude lower because of the higher viscosities; this would make an observation of any growth virtually impossible. Moreover, if the tentatively introduced phase line in Figure 2 is correct, the 70% solutions would be stable at temperatures above 255 K.

**Process of Growing.** An assessment of the rate determining process can be made by equating the flux in a stationary diffusion process to the flux needed for the observed growth. As a model, one may assume that what one sees growing is a sphere (or column, as the case may be) of low water concentration, in an environment of higher water content, and hence with an observable contrast. Water in the shell around that sphere diffuses to surrounding regions of ice. The observed speed of growth,  $3 \times 10^{-3} \text{ s}^{-1}$  for  $d(V/V_0)/dt$  in a 60 wt % PVP solution cooled to 248 K, requires a flux of  $10^{-8} \text{ kg m}^{-2} \text{ s}^{-1}$  of water. A diffusion current set up in a stationary field, caused by a free energy difference  $\Delta F$  of  $0.2 \text{ kJ mol}^{-1}$  over a distance of 100 nm and a diffusion constant of  $10^{-9} \text{ m}^2 \text{ s}^{-1}$ , has, however, an order of magnitude of  $1 \text{ kg m}^{-2} \text{ s}^{-1}$ . Therefore, the picture of larger volumes, like spheres, losing water to the surrounding medium through their entire surface cannot be correct. The effective interface through which the water escapes is obviously smaller than the actual surface; the ice that forms may have only very limited contacting surfaces with the dehydrating PVP solutions.

## Conclusions

The experimental observations have elucidated a couple of questions about the “unfreezable” water of 60–80 wt % PVP–water solutions.

First of all, the large amount of rapidly appearing and disappearing sharp peaks in the small-angle X-ray scattering region that have now been observed confirms their origin. These peaks are caused by patterns of columns arranged in a hexagonal symmetry. The basic length varies around 43 nm. Occasionally, such patterns extend over such large regions in space that very sharp interference lines result. The relatively high number of peaks with high Miller indices, corresponding with small interplanar distances, suggests that the patterns are formed by divisions in the continuum of the solution, rather than by assemblies of independent units.

A second aspect is the time dependent increase and shift to smaller  $q$  values of the intensity of the scattering, when time averaged. It became clear that, although the solutions at temperatures above 261 K may be in equilibrium, at lower temperatures they are certainly not. We quantified the changes in the scattering intensity and compared the result with theoretical predictions for different types of phase transitions. We did not find any indication that the hexagonal columns were involved in such a transition. A scaling procedure provided us with a single length, characteristic for each scattering spectrum. Those lengths appear to grow proportional with time to the power  $1/3$ . The speed of volume growth increases about linearly with decreasing temperature. The experimental observations are consistent with a slow first-order phase separation into ice and a more concentrated PVP solution. That concentration could be estimated by the use of a Flory–Huggins model for polymer solutions; it should be about 80 wt %. The liquidus in Figure 2 should proceed from 60 wt %, 262 K, to 80 wt %, 248 K, approximately as indicated. A comparison of the observed speed of growth with possible speed determining diffusion scenarios shows that there must be other, kinetic or geometric mechanisms that inhibit the growth besides the effect of the high viscosity.

The patterns of PVP of low water content can only grow as fast as the water can be implemented in the ice crystals. It has been shown experimentally<sup>15</sup> as well as by simulations<sup>16</sup> that polymer molecules adsorb preferentially on specific planes of the ice crystals. It seems, for instance, that glycopeptides in fish prevent ice crystal growth, because such peptides adsorb on pyramidal or secondary prism planes. This inhibits further attachment of water molecules to such planes. The growth of ice crystals might be impeded by adsorbed PVP in the same way. Putting it differently, the interface free energy between polymer solution and the growing ice crystal may be very different for different planes. This will result in the growth of the crystal in certain preferred directions.

We found a qualitative support for this conclusion in the simultaneous measurement of the wide-angle part of the scattering spectrum. A 60 wt % PVP solution, at a temperature of 265 K, shows a wide band of scattering intensity around  $q = 17 \text{ nm}^{-1}$ . It is the combined, isotropic scattering of the 0.3–0.4 nm distances in the liquid water–PVP mixture. During the 2 h run at a quench temperature of 253 K, this band loses about 40% of its intensity, whereas occasionally sharp peaks characteristic for ice do appear. This observation does not allow us to make any quantitative conclusion, but clearly the (103) reflection appears more often than can be expected for a polycrystalline ice sample of random orientation. The {103} planes could well be overabundant, because they act as receptors for the water coming in. The result would be the formation of elongated ice structures. At the same time, this might severely limit the transfer of water from the solution to the ice phase. The slowness of the process is therefore caused not only by the high viscosity but also by the same mechanism that is responsible for the formation of the hexagonal structures. In this respect the formation of these structures is connected with the phase transition; it impedes the transition and hides it.

**Acknowledgment.** This work was made possible by financial support from NWO, The Netherlands Organization for Scientific Research, help from the Foundation for Fundamental Research on Matter (FOM), and the facilities offered by the European Synchrotron Radiation Facility (ESRF) in Grenoble (France), in particular the Dutch–Belgian beam line (DUBBLE). We want to thank the staff of DUBBLE for the assistance that we received, in particular Wim Bras for his continuing and most stimulating support of this enterprise, and D. Bonn of the laboratoire de Physique Statistique de l’Ecole Normale Supérieure, Paris, for kindly placing viscosity data at our disposal.

## References and Notes

- (1) Franks, F. In *Water, a comprehensive treatise*, Vol 7; Franks, F., Ed.; Plenum Press: New York, 1982.
- (2) MacKenzie, A. P.; Rasmussen, D. H. In *Water structure at the water-polymer interface*; Jellinek, H. H. G., Eds.; John Wiley: New York, 1972.
- (3) Van der Elsken, J.; Bras, W.; Michielsen, J. C. F. *J. Appl. Cryst.* **2001**, *34*, 62.
- (4) Bras, W. *J. Macromol. Sci., Phys.* **1989**, *B37* (4), 557.
- (5) Caffrey, J. *Biochemistry* **1985**, *24*, 4826.
- (6) Nicolis, G.; Prigogine, I. *Self-Organization in Nonequilibrium Systems*; John Wiley: New York, 1967.
- (7) von Neumann, J. *Metal interfaces*; American Society for Metals: Cleveland, OH, 1952.
- (8) Strobl, R.; Schneider, M. *J. Polym. Sci.: Polym. Phys. Ed.* **1980**, *13*, 343.
- (9) Hentschel, M.; Hosemann, R. *Mol. Cryst. Liq. Cryst.* **1983**, *94*, 291.

- (10) Ceve, G.; Marsh, D. *Phospholipid Bilayers*; John Wiley: New York, 1987.
- (11) Mariani, P.; Rustichelli, F. In *Phase Transitions in Liquid Crystals*; Martellucci, S., Chester, A. N., Eds.; Plenum Press: New York, 1992; p 447.
- (12) Gunton, J. D.; San Miguel, M.; Sahni Paramdeep, S. In *Phase transitions and critical phenomena*; Domb, C., Lebowitz, J. L., Eds.; Academic Press: New York, 1983.

- (13) Lifshitz, I. M.; Slyosov, V. V. *J. Phys. Chem. Solids* **1961**, 19, 35.
- (14) Doi, M. *Introduction to Polymer Physics*; Clarendon Press: Oxford, U.K., 1996.
- (15) Knight, C. A.; Cheng, C. C.; Devries, A. L. *Biophys. J.* **1991**, 59, 409.
- (16) Lai, M.; Clark, A. H.; Lips, A.; Ruddock, J. N.; White, D. N. J. *Faraday Discuss.* **1993**, 95, 299.